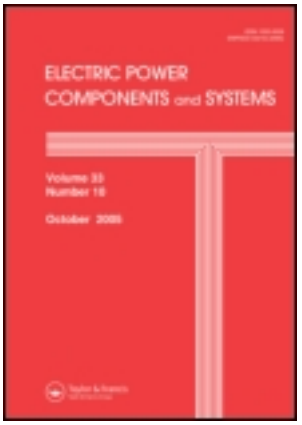

Electric Power Components and Systems
Publication details, including instructions for authors and subscription information:
http://www.tandfonline.com/loi/uemp20

Intelligent Linear-Quadratic Optimal Output Feedback Regulator for a Deregulated Automatic Generation Control System

Elyas Rakhshani [a]

[a] Electrical Engineering Department, Islamic Azad University, Gonabad Branch, Iran

Available online: 29 Feb 2012

To cite this article: Elyas Rakhshani (2012): Intelligent Linear-Quadratic Optimal Output Feedback Regulator for a Deregulated Automatic Generation Control System, Electric Power Components and Systems, 40:5, 513-533

To link to this article: http://dx.doi.org/10.1080/15325008.2011.647239

Electric Power Components and Systems, 40:513–533, 2012

ISSN: 1532-5008 print/1532-5016 online
DOI: 10.1080/15325008.2011.647239

Taylor & Francis
Taylor & Francis Group

Intelligent Linear-Quadratic Optimal Output Feedback Regulator for a Deregulated Automatic Generation Control System

ELYAS RAKHSHANI[1]

[1]Electrical Engineering Department, Islamic Azad University, Gonabad Branch, Iran

Abstract *One of the main observed problems in the control of automatic generation control systems is the limitation to access and measurement of state variables in the real world. In order to solve this problem, an optimal output feedback method, the linear-quadratic regulator controller, is used. In the output feedback method, only measurable state variables within each control area are required to use for feedback. But in order to improve dynamic performance and provide a better design for this controller, the concept of an intelligent regulator is added to the linear-quadratic regulators; as a result, the particle swarm optimization based linear-quadratic output feedback regulator and the imperialist competitive algorithm based linear-quadratic output feedback are proposed to calculate the global optimal gain matrix of controller intelligently. The optimal control law of this controller must be determined by minimizing a performance index under the output feedback conditions leading to coupled matrix equations. In conventional methods, the control law is handled by pole placement, iterative, or trial-and-error methods for choosing controller gains; thus, intelligent optimization techniques are applied to solve this problem. The proposed controllers are tested on a two-area automatic generation control power system, and a complete comparison between the proposed output feedback controllers with adaptive weighted particle swarm optimization, particle swarm optimization, the imperialist competitive algorithm, and a conventional output feedback controller is presented. The results show that the proposed intelligent controller improved the dynamic response of the system faster than the conventional controller and provided a control system that satisfied the load frequency control requirements.*

Keywords deregulated automatic generation control system, imperialist competitive algorithm, optimal output feedback, particle swarm optimization

1. Introduction

In a power system, any sudden load perturbation causes the deviation of tie-line exchanges and frequency fluctuations. Automatic generation control (AGC) plays a key role in this condition.

Based on the traditional vertical framework of power system utilities, the main goals of AGC are to maintain the frequency of each area and tie-line power flow within specified tolerance. The concept of conventional AGC was discussed and well known in [1–5]. With the deregulation of electric markets, AGC requirements should be expanded to

Received 7 June 2011; accepted 2 December 2011.
Address correspondence to Mr. Elyas Rakhshani, No. 2, 27th Sayyad Shirazi Ave., Vakil Abad Bolv., 91799-99497 Mashhad, Iran. E-mail: elyas.rakhshani@gmail.com

Nomenclature

apf	area participation factor
B	frequency bias
d_n	total demand
gpf	generator participation factor
K_i	integration controller gain
K_P	power system equivalent gain
R	droop characteristic
T_{12}	tie-line synchronizing coefficient between areas
T_G	time constant of governor
T_P	power system equivalent time constant
T_T	time constant of turbine
$T_{T\text{-}G}$	approximated time constant of turbine–governor set
ΔP_d	area load disturbance
ΔP_{Lj-i}	contracted demand of distribution company
ΔP_{Loc}	total local contracted demand
ΔP_{Mj-i}	power generation of generation company
ΔP_{tie}	net tie-line power flow
$\Delta P_{tie,actual}$	tie-line real power
$\Delta P_{tie,error}$	tie-line power error
ΔP_{ULj-i}	uncontracted demand
ζ	scheduled power tie-line power flow deviation

include the planning functions that are necessary to insure the resources needed for load frequency control (LFC) implementation in a competitive environment. In a deregulated scheme, LFC in a deregulated electricity market should be designed for different types of possible transactions. So a lot of studies try to modify the conventional LFC system to take into account the effect of bilateral contracts on the dynamics [6, 7] and improve the dynamical transient response of the system under competitive conditions [8–14].

To improve the transient response, various control strategies, such as linear feedback, optimal control, and the Kalman estimator method, have been proposed [8, 9]. There has been continuing efforts toward designing LFC with better performance using intelligence algorithms or robust methods [10–12]. In [13, 14], a fully controllable and observable state-space model was used to determine the optimal feedback gain for a quadratic regulator. Based on previous works in this field, it is very important to note that the main potential problem is that a "plant" is hardly ever linear with precisely known parameters. Therefore, some robustness against parameter variations/uncertainty must be built in during control design. In addition to this, the states of a system can have some physical meaning (*e.g.*, integration of area control error [ACE]), but sometimes they have no physical interpretation at all. Consequently there may be difficulty in obtaining the states to use for feedback. Based on all of these limitations, it is clear that using various methods, such as the robust method or observers, will increase the cost of system dramatically and makes the system even more complex. Also, in conventional methods, the control law is handled by pole placement, iterative, or some trial-and-error methods for choosing the controller gains. So, a kind of output feedback controller with intelligent optimization techniques should be applied to solve these problems.

In this article, as some of the states in the AGC model are not measurable, an optimal output feedback controller has been designed to use measurable state variables within each area for feedback. In fact, one of the main observed problems in the control of AGC systems is the limitation to access and measurement of state variables in the real world. So with a practical point of view, an optimal output feedback method, such as a linear-quadratic regulator (LQR) controller, is used to solve this problem. In the output feedback method, only the measurable state variables within each control area are required to use for feedback. The optimal control law is determined by minimizing a performance index under the output feedback conditions leading to coupled matrix equations. To solve these coupled equations, an iterative algorithm as a conventional method is used [13]. Usually, in conventional methods, the control law is handled by pole placement, iterative, or some trial-and-error methods for choosing the controller gains. But in order to enhance the performance of the system by minimizing the overshoot and steady-state error, and for more accuracy and better design for this LQR controller, intelligent optimization techniques, such as adaptive weighted particle swarm optimization (AWPSO) and the imperialist competitive algorithm (ICA), are applied to find the global optimal gain matrix.

The proposed controllers are tested on a two-area AGC power system, and a complete comparison between proposed output feedback controllers with AWPSO, particle swarm optimization (PSO), the ICA, and a conventional output feedback controller is presented. From the simulation results, the very useful controller design for the AGC control system has been realized by the intelligent-based linear-quadratic (LQ) regulator. It should be noted that the proposed methods are useful not only for optimal control of the LFC problem but also for other difficult problems.

2. Development of Deregulated AGC System

There are crucial differences between the AGC operation in a vertically integrated industry and a horizontally integrated industry. In the reconstructed power system after deregulation, operation, simulation, and optimization have to be reformulated, although the basic approach to AGC has been kept the same. The power system is assumed to contain two areas, and each area includes two generation companies (GENCOs) and also two distribution companies (DISCOs). But to understand how these contracts are implemented, the concept of the augmented generation participation matrix (AGPM) will be used [11]. The AGPM shows the participation factor of a GENCO in the load following contract with a DISCO. The rows and columns of the AGPM equal the total number of GENCOs and DISCOs in the overall power system, respectively. So, the AGPM structure for a large-scale power system with N control areas is given by

$$AGPM = \begin{bmatrix} AGPM_{11} & \cdots & AGPM_{1N} \\ \vdots & \ddots & \vdots \\ AGPM_{N1} & \cdots & AGPM_{NN} \end{bmatrix},$$

where

$$AGPM_{ij} = \begin{bmatrix} gpf_{(s_i+1)(z_j+1)} & \cdots & gpf_{(s_i+1)(z_j+m_j)} \\ \vdots & \ddots & \vdots \\ gpf_{(s_i+n_i)(z_j+1)} & \cdots & gpf_{(s_i+n_i)(z_j+m_j)} \end{bmatrix}.$$

In the above, n_i and m_i are the number of GENCOs and DISCOs in area i and gpf_{ij} refers to the generation participation factor and shows the participation factor of GENCO$_i$ in the total load following requirement of DISCO$_j$ based on the possible contract. The sum of all entries in each column of an AGPM is unity. The diagonal sub-matrices of an AGPM correspond to local demands, and off-diagonal sub-matrices correspond to demands of DISCOs in one area on GENCOs in another area. The details and block diagram of the generalized AGC for a two-area deregulated power system are shown in Figure 1. Dashed lines show interfaces between areas and the demand signals based on the possible contracts. These new information signals are absent in the traditional LFC scheme. As there are many GENCOs in each area, the ACE signal has to be distributed among them due to their ACE participation factor in the LFC task and $\sum_{j=1}^{n_i} apf_{ji} = 1$. The following can be written [13]:

$$d_i = \Delta P_{Loc,i} + \Delta P_{di}, \tag{1}$$

where

$$\Delta P_{Loc,i} = \sum_{j=1}^{m_i} \Delta P_{Lj-i}, \qquad \Delta P_{di} = \sum_{j=1}^{m_i} \Delta P_{ULj-i}, \tag{2}$$

$$\varsigma_i = \sum_{\substack{k=1 \\ k\neq 1}}^{N} \Delta P_{tie,ik,scheduled}, \tag{3}$$

$$\eta_i = \sum_{\substack{j=1 \\ j\neq 1}}^{N} T_{ij}.\Delta f_j, \tag{4}$$

$$\Delta P_{tie,ik,scheduled} = \sum_{j=1}^{n_i}\sum_{t=1}^{m_k} apf_{(s_i+j)(z_k+t)} \Delta P_{Lt-k} - \sum_{t=1}^{n_k}\sum_{j=1}^{m_i} apf_{(s_k+t)(z_i+j)} \Delta P_{Lj-i}, \tag{5}$$

$$\Delta P_{tie,i,error} = \Delta P_{tie,i,actual} - \zeta_i, \tag{6}$$

$$\Delta P_{m,k-i} = \rho_{ki} + apf_{ki} \sum_{j=1}^{m_i} \Delta P_{ULj-i} \qquad (k = 1, 2, \ldots, n_i), \tag{7}$$

$$\rho_{ki} = \sum_{j=1}^{N} \left[\sum_{t=1}^{m_j} gpf_{(s_i+k)(z_j+t)} \Delta P_{Lt-j} \right]. \tag{8}$$

Also, the error signal in Eq. (6) is used to generate its ACE signals in the steady state as follows:

$$ACE_i = B_i \Delta f_i + \Delta P_{tie,i,error}. \tag{9}$$

To illustrate the effectiveness of the proposed control design, a two control area power system is considered as a test system. It is assumed that each control area includes

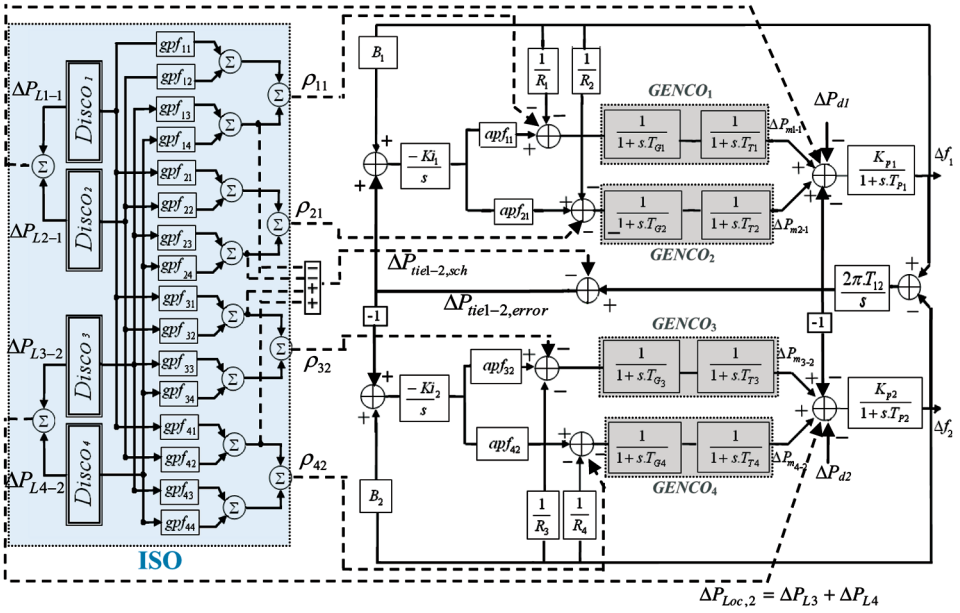

Figure 1. Modified LFC system in a deregulated environment for this study. (color figure available online)

two GENCOs and DISCOs, and the closed-loop system in Figure 1 is characterized in state-space form as follows:

$$\dot{x} = Ax + B.u, \qquad x(t_0) = x_0, \tag{10}$$

$$y = C.x, \tag{11}$$

where x is the state vector, and u is the vector of power demands of the DISCOs;

$$x = \Big[\Delta f_1 \quad \Delta f_2 \quad \Delta P_{m1-1} \quad \Delta P_{m2-1} \quad \Delta P_{m3-2} \quad \Delta P_{m4-2} \quad \int ACE_1 \quad \int ACE_2 \quad \Delta P_{tie1\text{-}2,actual}\Big]^T, \tag{12}$$

$$u = [\Delta P_{L1-1} \quad \Delta P_{L2-1} \quad \Delta P_{L3-2} \quad \Delta P_{L4-2} \quad \Delta P_{d1} \quad \Delta P_{d2}]^T.$$

The deviation of frequency, turbine output, and tie-line power flow within each control area are measurable outputs and other states such as governor outputs and the integration of the ACE is not measurable.

3. Design of Proposed Method for LFC System

The design of optimal control systems is an important function of control engineering. The purpose of the design is to realize a system with practical components that will provide the desired operating performance [15]. In this section, in order to improve the dynamic performance of system, and for more accuracy and better design for the conventional

LQR controller, a kind of intelligent techniques is added to find the global optimal gain matrix. Brief theories of these methods are described in this section.

3.1. *Overview of Optimal Output Feedback*

For the system that is defined by Eqs. (11) and (12), the output feedback control law is [15]

$$u = -K.y. \tag{13}$$

The objective of this regulator for the system may be attained by minimizing a performance index (J) of the type

$$J = 1/2 \int [x^T(t).Q.x(t) + u^T(t).R.u(t)]\ dt. \tag{14}$$

By substituting Eq. (13) into Eq. (11), the closed-loop system equation is

$$\dot{x} = (A - BKC)x = A_c.x. \tag{15}$$

This dynamical optimization may be converted to an equivalent static one that is easier to solve, as follows. So a constant, symmetric, positive-semi definite matrix P can be defined as

$$d(x^T Px)/dt = -x^T(Q + C^T K^T RKC)x, \tag{16}$$

$$J = 1/2.x^T(0)Px(0) - 1/2 \lim_{t\to\infty} x^T(t)P.x(t). \tag{17}$$

Assuming that the closed-loop system is stable so that $x(t)$ vanishes with time, this becomes

$$J = 1/2.x^T(0)Px(0). \tag{18}$$

If P satisfies Eq. (16), Eq. (15) may be used to see that

$$\begin{aligned} -x^T(Q + C^T K^T RKC)x &= d(x^T Px)/dt = \dot{x}^T Px + x^T P\dot{x} \\ &= x^T \left(A_c^T P + PA_c\right) x, \end{aligned} \tag{19}$$

$$g \equiv A_c^T P + PA_c + C^T K^T RKC + Q = 0, \tag{20}$$

Equation (18) may be written as

$$J = 1/2.tr(PX), \tag{21}$$

where the $n \times n$ symmetric matrix X is defined as

$$X = E\{x(0).x^T(0)\}. \tag{22}$$

So the best K must be selected to minimize Eq. (14) subject to the constraint in Eq. (20) on the auxiliary matrix P. To solve this modified problem, the Lagrange multiplier approach will be used, and the constraint will be adjoined by defining this Hamiltonian:

$$H = tr(PX) + tr(gS). \tag{23}$$

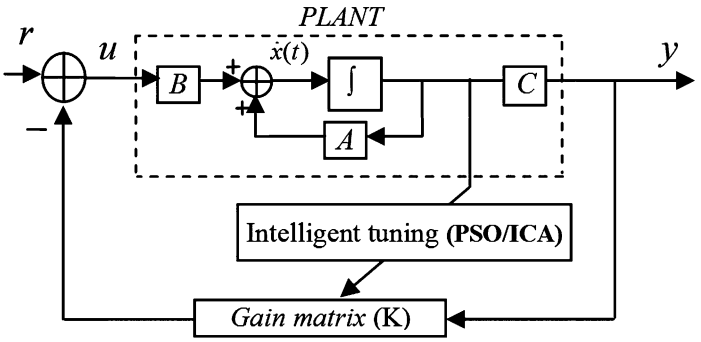

Figure 2. Closed-loop system with the proposed LQR output feedback controller.

Now to minimize Eq. (21), partial derivatives of H with respect to all the independent variables P, S, and K must be equal to zero:

$$0 = \partial H/\partial S = A_c^T P + PA_c + C^T K^T RKC + Q, \tag{24}$$

$$0 = \partial H/\partial P = A_c S + SA_c^T + X, \tag{25}$$

$$0 = 1/2.(\partial H/\partial K) = RKCSC^T - B^T PSC^T. \tag{26}$$

To obtain the output feedback gain K with minimizing Eq. (14), three coupled equations (Eqs. (24), (25), and (26)) must be solved simultaneously. The first two of these are Lyapunov equations, and the third is an equation for gain K. If R is positive definite and non-singular, then Eq. (26) may be solved for K [15]:

$$K = R^{-1}B^T PSC^T(CSC^T)^{-1}. \tag{27}$$

Various methods may be used to solve these equations, such as iterative methods [13]. But, as shown in Figure 2, the PSO and ICA algorithms are used to find the global optimal gain matrix.

3.2. AWPSO Algorithm

PSO is a population-based heuristic search technique that imitates the finding-food principle of a bird swarm [16, 17]. A swarm consists of a set of particles, where each particle represents a potential solution within the search space. Particles are then flown through the hyperspace, where the position of each particle is changed according to its own experience and that of its neighbors. Let $\vec{x}_i(t)$ denote the position of particle P_i in hyperspace at time step t. The position of P_i is then changed by adding a velocity $\vec{v}_i(t)$ to the current position as

$$\vec{x}_i(t) = \vec{x}_i(t-1) + \vec{v}_i(t). \tag{28}$$

The velocity vector drives the optimization process and reflects the socially exchanged information. The velocity update equation is as follows:

$$v_i(t) = \omega.v_i(t-1) + c_1.r_1(P_{bi} - x_i(t-1)) + c_2.r_2(P_g - x_i(t-1)), \tag{29}$$

where w is the inertia weight, c_1 and c_2 are positive constants, and r_1 and r_2 are random numbers obtained from a uniform random distribution function in the interval [0, 1].

The parameters $\vec{P}_{bi}$ and $\vec{P}_g$ represent the best previous position of the ith particle and the position of the best particle among all particles in the population, respectively [17]. The inertia weight controls the influence of previous velocities on the new velocity. Large inertia weights cause a larger exploration of the search space, while smaller inertia weights focus the search on a smaller region. Typically, PSO started with a large inertia weight, which is decreased over time. But in this article, for more adaption, the following formula is used to change the inertia weight at each generation:

$$w = w_0 + r(1 - w_0), \tag{30}$$

where w_0 is the initial positive constant in the interval [0, 1], and r is random number obtained from a uniform random distribution function in the interval [0, 1].

The suggested range for w_0 is [0, 0.5], which makes the weight w randomly varying between w_0 and 1. As shown in Figure 3, to improve the performance of the PSO, Mahfouf *et al.* [18] proposed an AWPSO algorithm, in which the velocity in Eq. (29) is modified as follows:

$$v_i(t) = \omega.v_i(t-1) + \alpha.[c_1.r_1(P_{bi} - x_i(t-1)) + c_2.r_2(P_g - x_i(t-1)]. \tag{31}$$

The second term in Eq. (32) can be viewed as an acceleration term, which depends on the distances between the current position $\vec{x}_i(t)$, the personal best $\vec{P}_{bi}$, and the global best $\vec{P}_g$. The acceleration factor α is defined as follows:

$$\alpha = \alpha_0 + t/T, \tag{32}$$

where t is the current generation, T denotes the number of generations, and the suggested range for α_0 is [0.5, 1].

As can be seen from Eq. (31), the acceleration term will increase as the number of iterations increases, which will enhance the global search ability at the end of a run and help the algorithm to jump out of the local optimum.

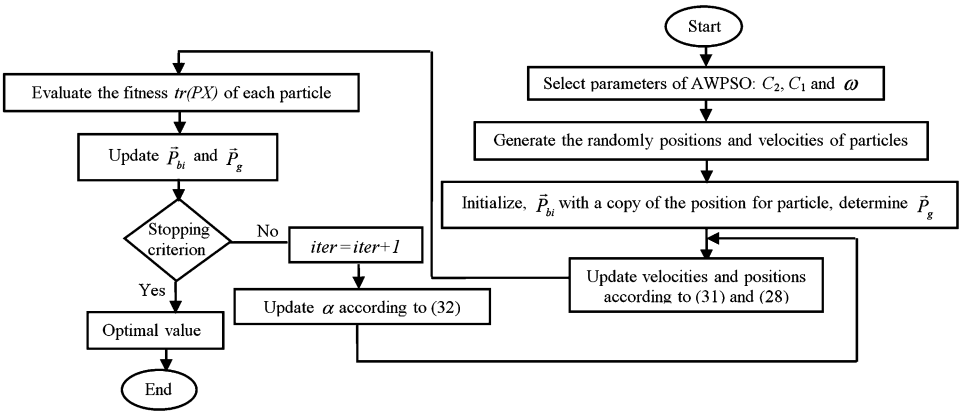

Figure 3. Flowchart of the proposed AWPSO technique.

3.3. ICA

The ICA was proposed by Atashpaz and Lucas [19] and Lucas *et al.* [20], and it was inspired by imperialist competition. The ICA is a socio-politically motivated optimization algorithm that is similar to many other evolutionary algorithms, and it starts with a random initial population or empires. Each individual agent of an empire is called a country, and the countries are categorized into two types—colony and imperialist state—that collectively form empires. Imperialistic competitions among these empires form the basis of the ICA. During this competition, weak empires collapse and powerful ones take possession of their colonies. Imperialistic competitions converge to a state in which there exists only one empire, and its colonies are in the same position and have the same cost as the imperialist [19].

With an N-dimensional optimization problem, a country is a $1 \times N$ array. This array is defined as follows:

$$Country = [p_1, p_2, p_3, \ldots, p_N]. \tag{33}$$

Each variable in the country can be interpreted as a socio-political characteristic of a country. From this point of view, all the algorithm does is to search for the best country that is the country with the best combination of socio-political characteristics, such as culture and language. From an optimization point of view, this leads to finding the optimal solution of the problem and solution with the least cost value. The cost of a country is found by the evaluation of the cost function for all variables:

$$cost = f(country) = f(P_1, P_2, P_3, \ldots, P_N). \tag{34}$$

To form the initial empires, the colonies are divided among imperialists based on their power. That is, the initial number of colonies of an empire should be directly proportionate to its power. To proportionally divide the colonies among imperialists, the normalized cost of an imperialist is defined by [19]

$$C_n = c_n - \max_i\{c_i\}, \tag{35}$$

where c_n is the cost of the nth imperialist, and C_n is its normalized cost. Having the normalized cost of all imperialists, the normalized power of each imperialist is defined by

$$P_n = \left| \frac{C_n}{\sum_{i=1}^{N} C_i} \right|. \tag{36}$$

Then the initial number of colonies ($N.C_{.n}$) of an empire is

$$N.C_{.n} = round\{p_n.N\}. \tag{37}$$

It is clear that bigger empires have a greater number of colonies, while the weaker ones have less. In general, in each term of the ICA, the following operations are conducted.

Assimilation of Colonies. Colonies of each imperialist are assimilated to their respective imperialist. Assimilation is formulated as follows:

$$x_{col}^{new} = x_{col}^{old} + \beta.r \otimes (x_{imp} - x_{col}^{old}), \tag{38}$$

where β is an assimilation factor, r is a vector, and its elements are uniformly distributed random numbers in $[0, 1]$. x_{imp}, x_{col}^{old}, and x_{col}^{new} are the position of the imperialist, the old position of the colony, and the new position of the colony, respectively. In [19], the new position of the colony is angularly deviated. To search different points around the imperialist, a random amount of deviation is added to the direction of movement. Figure 4 shows the new direction. In this figure, θ is a random number with uniform distribution. Then,

$$\theta \sim U(-\gamma, \gamma),$$

where γ is a parameter that adjusts the deviation from the original direction, and d is the distance between the colony and imperialist. A $\beta > 1$ causes the colonies to get closer to the imperialist. In these simulations, α and γ are 2 and $\pi/4$ (rad), respectively. For more information about deviation, refer to [19].

Revolution of Colonies. In this step, selected colonies of every imperialist are changed randomly or revolved. Revolution is applied to a colony, with a probability of p_r.

Exchange with Best Colony. If, after assimilation and revolution steps, there are colonies that are better than their respective imperialists, the imperialist is exchanged with its best colony. In other words, the imperialist will be the colony, and the best colony will be the new imperialist.

Imperialist Competition. The weakest imperialist among others loses its weakest colony. One of other imperialists will randomly capture the lost colony. The better the imperialist is, the greater the probability that it will possess the colony. An imperialist without a colony will collapse.

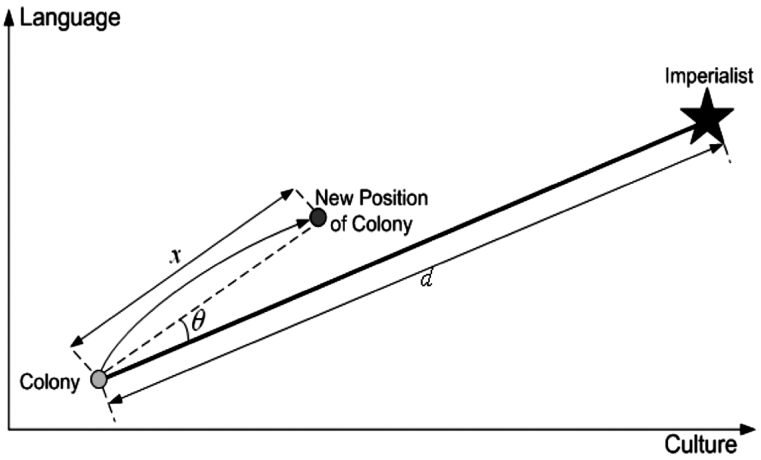

Figure 4. Moving colonies toward their relevant imperialist in a randomly deviated direction.

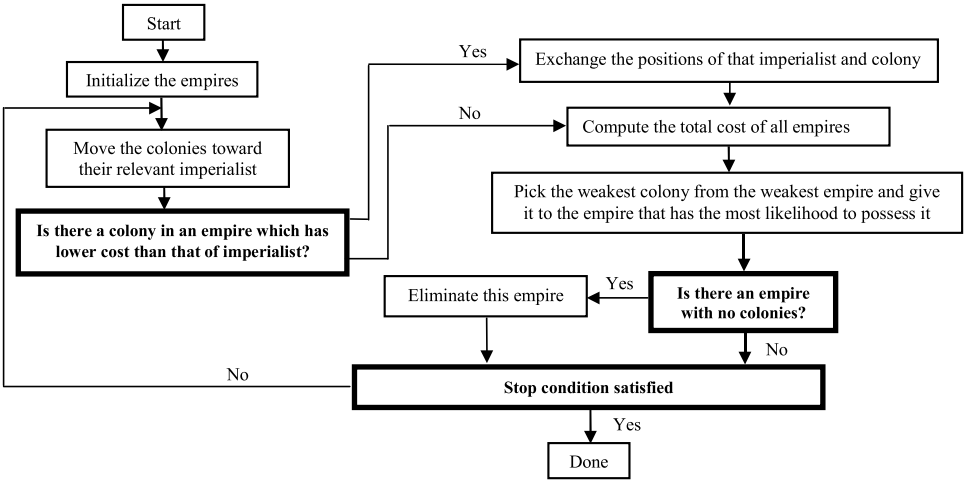

Figure 5. Flowchart of the ICA.

It will become a colony and captured by other imperialists. As shown in Figure 5, the mentioned steps are carried out, while stop conditions are not satisfied.

4. Simulation Results

In this section, the proposed control for a multi-area LFC system in Section 3 is simulated for a possible contracted scenario under various operating condition and large load demands. At this step, a conventional LQR output feedback is applied for a case study with two areas.

To examine the effectiveness of the proposed methods on the reduction of trajectory sensitivity to plant-parameter variations, system parameters (*i.e.*, GENCO parameters and control area parameters) are increased about 25%. Also in the simulation study, the linear model of each GENCO model in Figure 1 can be replaced by the non-linear model of Figure 6 (with ± 0.1 limit). This is to take the generation rate constraint (GRC) into account, *i.e.*, the practical limit on the rate of change in the generating power of each GENCO.

Finally, to gain a better design in the conventional LQR controller, two separate intelligent LQ controllers for the same scenario in an LFC system are studied. The first is based on a PSO-LQ controller, and the second is based on an ICA-LQ controller design. For the performance comparison in each study, the conventional controller

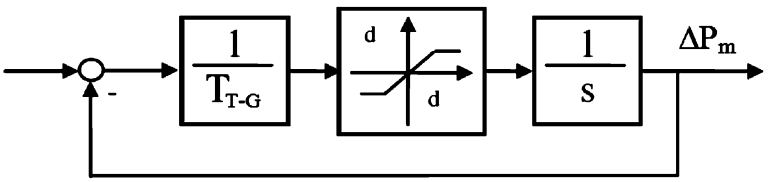

Figure 6. Non-linear GENCO model with GRC.

and a system without a controller are also simulated, and the results are presented separately. The simulations are done using MATLAB (The MathWorks, Natick Massachusetts, USA) platform [13], and the parameter values of the power system are given in Table 1.

Also it is assumed that DISCOs demand 0.1 p.u. MW total power from GENCOs, as defined by entries in following AGPM:

$$AGPM = \begin{bmatrix} 0.5 & 0.25 & 0 & 0.3 \\ 0.2 & 0.25 & 0 & 0 \\ 0 & 0.25 & 1 & 0.7 \\ 0.3 & 0.25 & 0 & 0 \end{bmatrix},$$

and each GENCO participates in AGC, as defined by following apf:

$$apf_1 = 0.75, \qquad apf_2 = 1 - apf_1 = 0.25,$$

$$apf_3 = 0.5, \qquad apf_4 = 1 - apf_3 = 0.5.$$

The performance index of optimal output feedback for the first study is given in Figure 7. Also, based on the information in Table 1, the linear time-invariant (LTI) dynamic model for the system shown in Figure 1 is given by

$$A = \begin{bmatrix} -0.0417 & 0 & 5.3125 & 5.3125 & 0 & 0 & -5.3125 & 0 & 0 \\ 0 & -0.0333 & 0 & 0 & 4.2 & 4.2 & 4.2 & 0 & 0 \\ -0.11153 & 0 & -2.1739 & 0 & 0 & 0 & 0 & -1.1413 & 0 \\ -0.1119 & 0 & 0 & -2.1978 & 0 & 0 & 0 & -0.3846 & 0 \\ 0 & -0.1171 & 0 & 0 & -2.2989 & 0 & 0 & 0 & -0.8046 \\ 0 & -0.1003 & 0 & 0 & 0 & -2.1277 & 0 & 0 & -0.7447 \\ 0.0390 & -0.0390 & 0 & 0 & 0 & 0 & 0 & 0 & 0 \\ 0.0846 & 0 & 0 & 0 & 0 & 0 & -1.0000 & 0 & 0 \\ 0 & 0.1262 & 0 & 0 & 0 & 0 & -1.0000 & 0 & 0 \end{bmatrix}_{9\times 9},$$

$$B = \begin{bmatrix} -5.3125 & -5.3125 & 0 & 0 \\ 0 & 0 & -4.2000 & -4.2000 \\ 1.0870 & 0.5435 & 0 & 0.6522 \\ 0.4396 & 0.5495 & 0 & 0 \\ 0 & 0.5747 & 2.2989 & 1.6092 \\ 0.6383 & 0.5319 & 0 & 0 \\ 0 & 0 & 0 & 0 \\ 0.3000 & 0.3000 & 0 & -0.3000 \\ -0.3000 & -0.5000 & 0 & 0.3000 \end{bmatrix}_{9\times 4},$$

$$C = \begin{bmatrix} 1 & 0 & 0 & 0 & 0 & 0 & 0 & 0 & 0 \\ 0 & 1 & 0 & 0 & 0 & 0 & 0 & 0 & 0 \\ 0 & 0 & 1 & 0 & 0 & 0 & 0 & 0 & 0 \\ 0 & 0 & 0 & 1 & 0 & 0 & 0 & 0 & 0 \\ 0 & 0 & 0 & 0 & 1 & 0 & 0 & 0 & 0 \\ 0 & 0 & 0 & 0 & 0 & 1 & 0 & 0 & 0 \\ 0 & 0 & 0 & 0 & 0 & 0 & 1 & 0 & 0 \end{bmatrix}_{7\times 9}.$$

Table 1
Parameters values of power system

	Area 1		Area 2	
GENCOs parameters				
T_T (sec)	0.4	0.375	0.375	0.4
T_G (sec)	0.075	0.1	0.075	0.0875
R (Hz/p.u.)	3	3.125	3.125	3.375
Control area parameters				
K_P (p.u./Hz)	127.5		127.5	
T_P (sec)	25		31.25	
B (p.u./Hz)	0.532		0.495	

4.1. AWPSO-LQR Simulation Results

First, PSO and AWPSO methods are used to solve the optimization problem. Based on the flowchart presented in Figure 3, the fitness function in PSO is equivalent to the objective function of Eq. (21) in the problem. The fitness function is evaluated, and the population is updated iteratively by Eqs. (28) and (31) until the optimum is obtained or the stopping criterion determines to finish the calculations. Population size is set to 50, and based on Figure 8, the maximum number of iterations is set to 100. Complete information about PSO parameters are presented in Table 2.

The performance index for the PSO algorithm is given in Figure 8, and simulation results for this part are shown in Figures 9–11. It is very important to note that the off-diagonal blocks of the AGPM correspond to the contract of a DISCO in one area with a

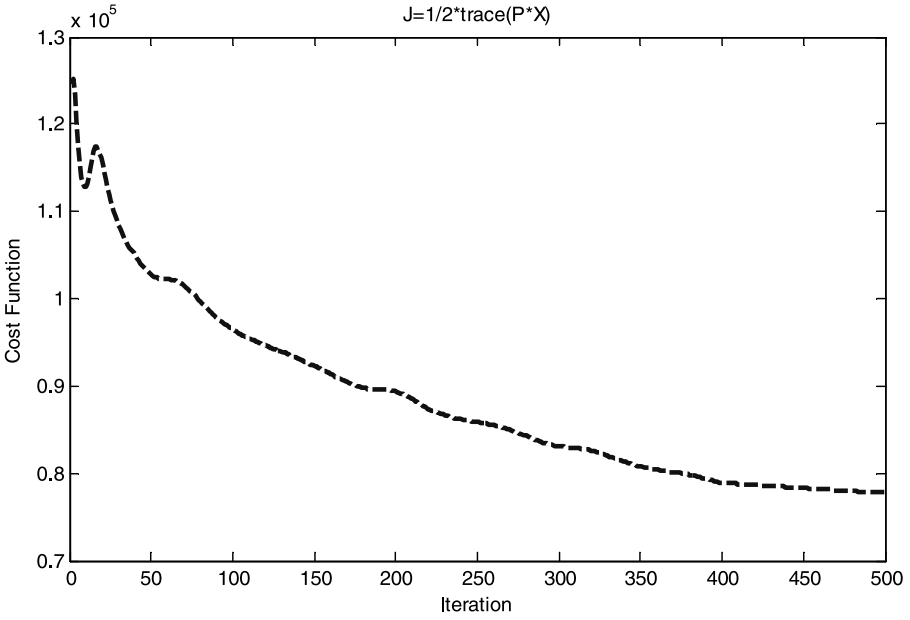

Figure 7. Performance index for the optimal output feedback.

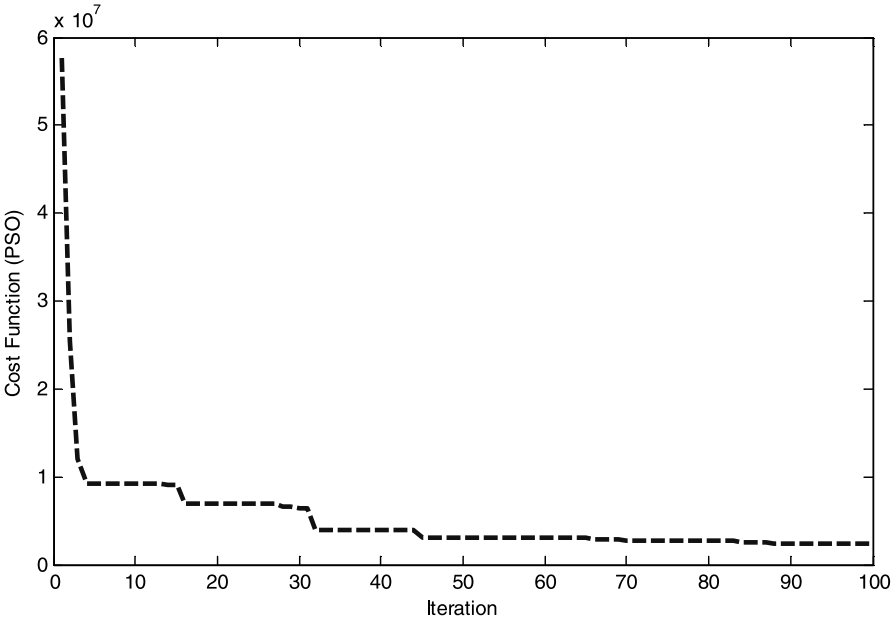

Figure 8. Convergence of the objective function in PSO algorithm.

GENCO in another area. So as Figure 9 shows, the tie-line power flow properly converges to the specified value of Eq. (1) in the steady state, *i.e.*, $\Delta P_{tie1\text{-}2,scheduled} = -0.05$ p.u. MW.

The frequency deviations of two areas are presented in Figures 10 and 11, respectively, and they also are compared with a conventional LQ output feedback regulator. It is clear that the initial system is unstable, and with using proposed methods, dynamic responses are improved effectively, and the frequency deviation of all areas and the tie-line power flows are quickly driven back to zero and have small overshoots.

4.2. ICA-LQR Simulation Results

In a similar manner to the previous method, the above optimization problem is solved by the ICA as the second approach. The simulation results are depicted in Figures 12–15. Convergence of the objective function in the ICA is shown in Figure 12, and it should be mentioned that different criteria can be used to stop the algorithm. One idea is to use a number of maximum iterations of the algorithm, called maximum decades,

Table 2
PSO parameters

Population size	50
C_1	1.8
C_2	1.8
w_0	0.4
$w_{\max}$	0.9
Number of iterations	100

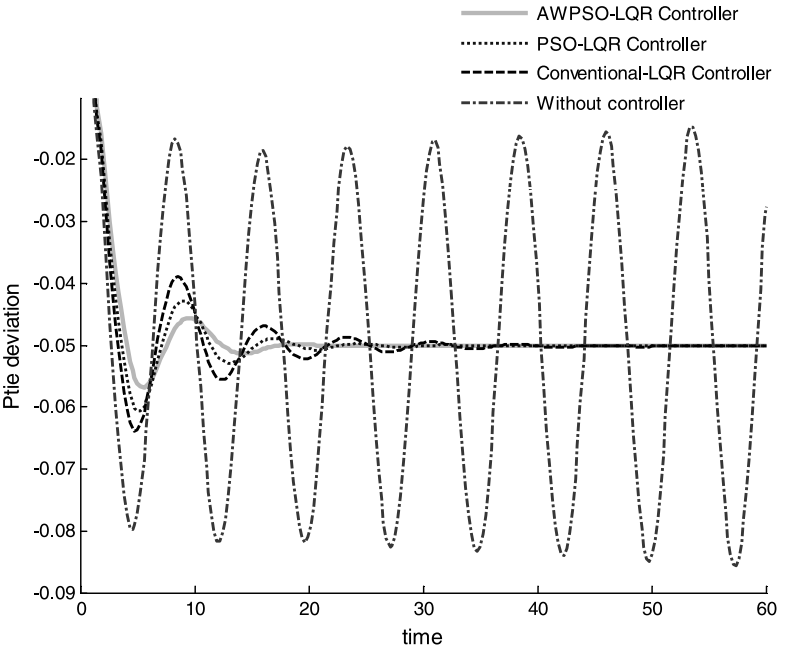

Figure 9. Deviation of tie line power flow (p.u. MW) and time (sec).

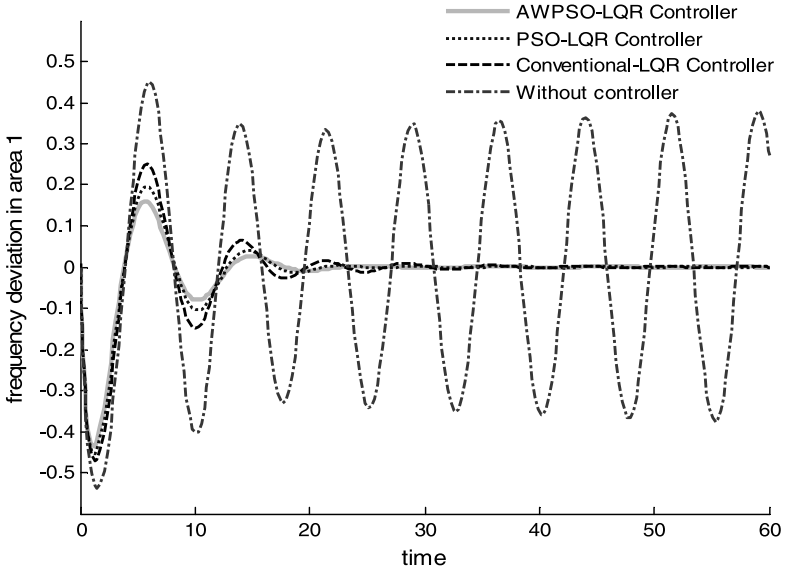

Figure 10. Frequency deviation in area 1 (rad/sec).

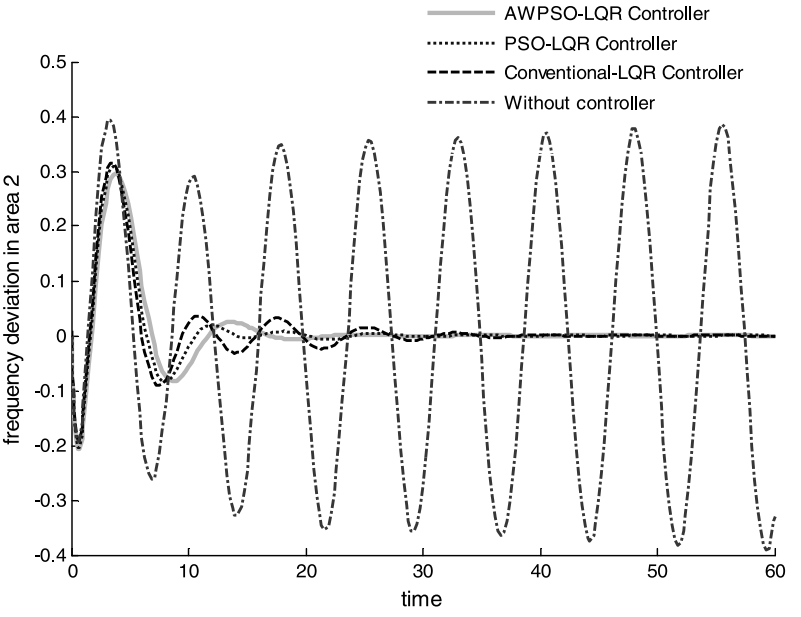

Figure 11. Frequency deviation in area 2 (rad/sec).

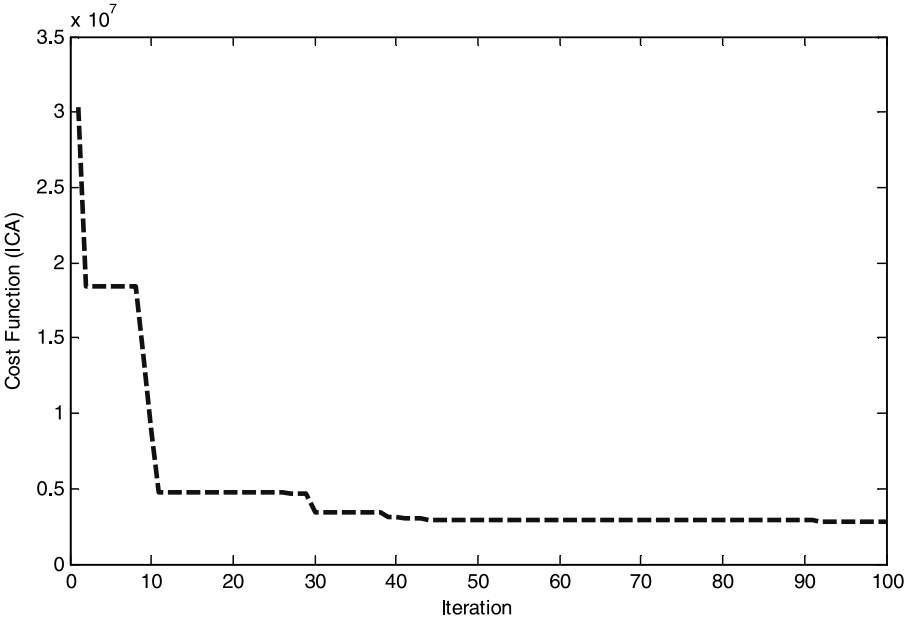

Figure 12. Convergence of the objective function in the ICA.

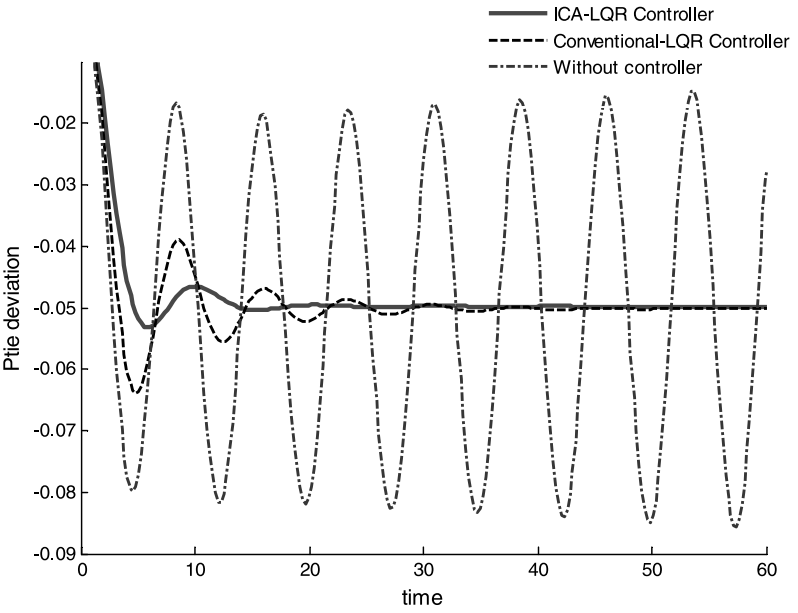

Figure 13. Deviation of tie line power flow (p.u. MW) and time (sec).

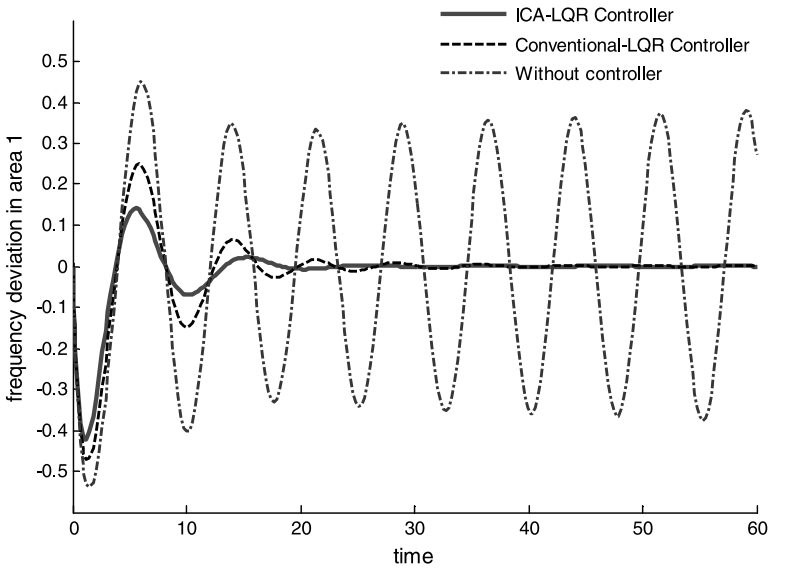

Figure 14. Frequency deviation in area 1 (rad/sec).

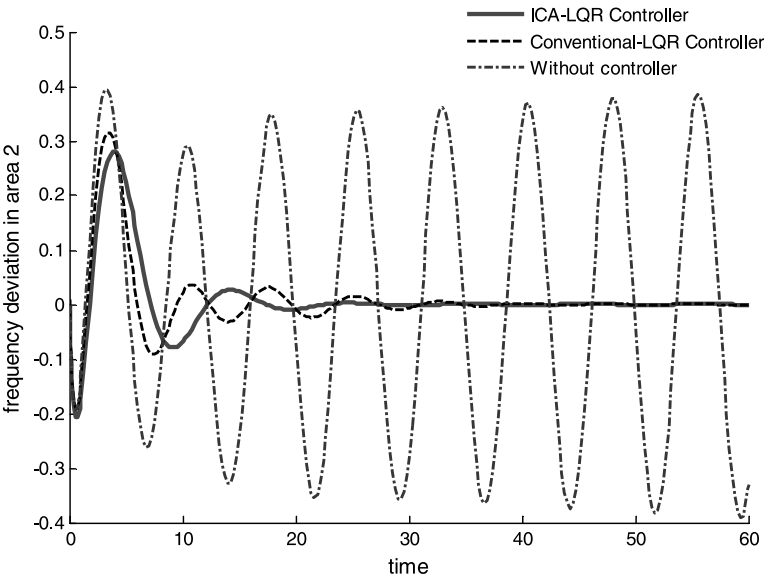

Figure 15. Frequency deviation in area 2 (rad/sec).

to stop the algorithm. Also, the end of imperialistic competition, when there is only one empire, can be considered as the stop criterion of the ICA. On the other hand, the algorithm can be stopped when its best solution in different decades cannot be improved for some consecutive decades. Complete information about ICA parameters are presented in Table 3.

Based on Figures 8 and 12, the proposed intelligent controllers with the ICA or PSO algorithm have fast convergences to decrease objective functions and, consequently, to improve the performance of the controller. The performance index of the conventional controller, as shown in Figure 8, is not the best solution for the problem. In order to verify the ICA's results, a comparison is made between the ICA-based controller and a conventional LQR controller. As shown in Figures 13–15, using this method, the frequency deviation of each area and the tie-line power have a good dynamic response in comparison with conventional controller. Also, for more evaluation and simulation discussion, eigenvalue analysis and dynamic result comparisons for each method are presented in Tables 4 and 5, respectively.

Dynamic results obtained from used algorithms are summarized in Table 4. It shows that intelligent LQ controllers have better performance as compared to the conventional

Table 3
ICA parameters

Initial countries	50
Initial imperialists	8
Revolution rate	0.35
α	2
Number of iterations	100

Table 4
Comparison of dynamic results

Controller	Settling times (sec)	Maximum overshoot (rad/s)
Conventional LQR	40.13	0.2362
PSO-LQR	34.31	0.1822
AWPSO-LQR	25.84	0.1227
ICA-LQR	28.42	0.1463

Table 5
Eigenvalue of the system

Modes	Without controller	Conventional	PSO based	AWPSO based	ICA based
Δf_1	$0.0029 + 0.83i$	$-0.1017 + 0.74i$	$-0.159 + 0.81i$	$-0.2419 + 0.794i$	$-0.3388 + 0.779i$
Δf_2	$0.0029 - 0.83i$	$-0.1017 - 0.74i$	$-0.159 - 0.81i$	$-0.2419 - 0.794i$	$-0.3388 - 0.779i$
ΔP_{m1}	$-0.201 + 0.60i$	$-0.2136 + 0.61i$	$-0.213 + 0.61i$	$-0.2149 + 0.617i$	$-0.2140 + 0.609i$
ΔP_{m2}	$-0.201 - 0.60i$	$-0.2136 - 0.61i$	$-0.213 - 0.61i$	$-0.2149 - 0.617i$	$-0.2140 - 0.609i$
ΔP_{m3}	-0.4758	-0.4975	-0.4762	-0.4948	-0.4638
ΔP_{m4}	-1.6640	-1.7273	-1.7579	-1.7481	-1.7687
$\int ACE_1$	-1.9190	-1.9326	-2.2426	-1.9586	-2.3071
$\int ACE_2$	-2.1849	-2.2425	-2.1833	-2.2601	-2.0028
ΔP_{tie}	-2.2316	-2.1842	-2.3201	-2.5841	-2.7855

LQR method. It is clear that the AWPSO-LQ controller has the smallest settling time of 25.84 sec, while the conventional LQR method has the lowest value with 40.13 sec. Also, the maximum overshoot ranges for AWPSO, PSO, and the ICA are 0.1227, 0.1822, and 0.1463, respectively, while the maximum overshoot for the conventional LQR controller is 0.2362, which is the largest value in the simulation results.

Also, Table 5 shows the eigenvalues of the power system described in Section 2 for this simulated case. It can be seen that two of the eigenvalues are on the right half of the s-plane and without any control making the system unstable. Using the proposed intelligent methods, the frequency deviation of all areas is quickly driven back to zero and has a good dynamic response.

5. Conclusion

In this article, a new design for an LQ optimal output feedback regulator for a deregulated LFC system is presented. In this way, an optimal output feedback method, such as an LQR controller, is used to overcome the limitation to access and measurement of state variables in the real world. The calculation of output feedback control gains is conventionally handled by trial-and-error or iteration methods. Thus, by adding the idea of an intelligent regulator, the problem of finding the global optimum gain matrices for a classic LQR controller has been formulated perfectly.

To solve this problem, three intelligent optimization methods are utilized: PSO, AWPSO, and the ICA. The proposed method has been applied to a multi-area LFC

system in a deregulated environment. In fact, in order to improve dynamic performance and provide a better design for output feedback controller, the concept of an intelligent regulator is added to the LQ regulators; as a result, the PSO-based LQ output feedback regulator and ICA-based LQ output feedback are proposed to calculate the global optimal gain matrix of the controller intelligently. Based on simulation results, convergence speeds in proposed intelligent methods are much better than a conventional LQR controller. Considering stability index, settling time, and maximum overshoots, the proposed methods have better performance in comparison with a conventional controller. Also, the results are shown that the proposed intelligent controller improved the dynamic response of the LFC system faster than a conventional controller and provides a control system that satisfied the LFC requirements. It should be noted that the proposed methods are useful not only for the optimal control of LFC problem but also for other difficult problems.

Acknowledgment

This research work has been supported by the Spanish Ministry of Science and Innovation under the project ENE2011-29041-C02-01.

References

1. Kundur, P., *Power System Stability and Control*, New York: McGraw-Hill, 1994.
2. Saadat, H., *Power System Analysis*, New York: McGraw-Hill, 1999.
3. Elgerd, O. I., and Fosha, C. E., "Optimum megawatt-frequency control of multi-area electric energy systems," *IEEE Trans. Power Apparatus Syst.*, Vol. PAS-89, pp. 556–563, April 1970.
4. Jaleeli, N., Van Slyck, L. S., Ewart, D. N., Fink, L. H., and Hoffman, A. G., "Understanding automatic generation control," *IEEE Trans. Power Syst.*, Vol. 7, No. 3, pp. 1106–1112, August 1992.
5. Doolla, S., Bhatti, T. S., and Bansal, R. C., "Load frequency control of an isolated small hydro power plant using multi-pipe scheme," *Elect. Power Compon. Syst.*, Vol. 39, No. 1, pp. 46–63, January 2011.
6. Kumar, J., Ng, K.-H., and Sheble, G., "AGC simulator for price-based operation. Part 1: A model," *IEEE Trans. Power Syst.*, Vol. 12, No. 2, pp. 527–532, May 1997.
7. Donde, V., Pai, A., and Hiskens, I. A., "Simulation and optimization in a AGC system after deregulation," *IEEE Trans. Power Syst.*, Vol. 16, No. 3, pp. 481–489, August 2001.
8. Liu, F., Song, Y.H., Ma, J., Mei, S., and Lu, Q., "Optimal load-frequency control in restructured power systems," *IEE Proc. Generat. Transm. Distribut.*, Vol. 150, No. 1, pp. 87–95, January 2003.
9. Rerkpreedapong, D., and Feliachi, A., "Decentralized load frequency control for load following services," *IEEE Power Eng. Soc. Winter Mtg.*, Vol. 2, No. 1, pp 1252–1257, January 2002.
10. Demiroren, A., and Zeynelgil, H. L., "GA application to optimization of AGC in three-area power system after deregulation," *Elect. Power Energy Syst.*, Vol. 29, No. 3, pp. 230–240, March 2007.
11. Shayeghi, H., Shayanfar, H. A., and Malik, O. P., "Robust decentralized neural networks based LFC in a deregulated power system," *Elect. Power Syst. Res.*, Vol. 77, pp. 241–251, April 2007.
12. Huddar, A., and Kulkarni, P. S., "A robust method of tuning a decentralized proportional-integral load frequency controller in a deregulated environment using genetic algorithms," *Elect. Power Compon. Syst.*, Vol. 37, No. 3, pp. 265–286, February 2009.
13. Rakhshani, E., and Sadeh, J., "Practical viewpoints on load frequency control problem in a deregulated power system," *Energy Conversion Manag.*, Vol. 51, No. 6, pp. 1148–1156, 2010.
14. Rakhshani, E., and Sadeh, J., "Reduced-order observer control for two-area LFC system after deregulation," *Control Intell. Syst.*, Vol. 38, No. 4, pp. 185–193, 2010.

15. Lewis, F. L., and Syrmos, V. L., *Optimal Control*, Englewood Cliffs, NJ: Prentice Hall, Chap. 4, 1995.
16. Soliman, H. M., Bayoumi, E. H. E., and Hassan, M. F., "Power system stabilizer design for minimal overshoot and control constraint using swarm optimization," *Elect. Power Compon. Syst.*, Vol. 37, No. 1, pp. 111–126, December 2008.
17. Jin, N., and Rahmat-Samii, Y., "Advances in particle swarm optimization for antenna designs: Real-number, binary, single- objective and multi-objective implementations," *IEEE Tran. Antennas Propagat.*, Vol. 55, No. 3, pp. 556–567, March 2007.
18. Mahfouf, M., Chen, M., and Linkens, D. A., "Adaptive weighted particle swarm optimisation (AWPSO) of mechanical properties of alloy steels," *8th International Conference on Parallel Problem Solving from Nature (PPSN VIII)*, Birmingham, UK, 18–22 September 2004.
19. Atashpaz, E., and Lucas, C., "Imperialist competitive algorithm: An algorithm for optimization inspired by imperialistic competition," *IEEE Congress on Evolutionary Computation*, pp. 4661–4667, Singapore, 25–28 September 2007.
20. Lucas, C., Nasiri-Gheidari, Z., and Tootoonchian, F., "Application of an imperialist competitive algorithm to the design of a linear induction motor," *Energy Conversion Manag.*, Vol. 51, No. 7, pp. 1407–1411, 2010.